

DEBRIS (Distributed Element Beamformer Radar for Ice and Subsurface Sounding)

and

DOWSER (Distributed Occluded Water Sensors using Electromagnetics in Reactive Regime)

Principal Investigator: Robert Beauchamp (334); Co-Investigators: Ala Khazendar (334), Bruno Quadrelli (347), Mark Haynes (334), Richard Hodges (337), Darmindra Arumugam (334), Paolo Focardi (337), Jack Bush (334), Rayan Mazouz (347), Peter Mao (334), Riccardo Apa (347), Stefano Aliberti (347), Gaurangi Gupta (337), Nicole Bienert (334)

Program: FY22 R&TD Strategic Initiative Strategic Focus Area: Radars 2030 Strategic Initiative Leader: Simone Tanelli

Objectives

The current state-of-the-art radar beamformers are physically constrained by the size of a single spacecraft or its deployable structures. For the **Distributed Element Radar Beamformer for Ice and Subsurface Sounding (DEBRIS)**, we focused on using multiple small spacecraft to synthesize antenna apertures on the order of kilometers in scale [A,B]. The coherent distributed array requires formation flying and position coordination of all spacecraft, and the relative position and timing between spacecraft must be known with precision of a small fraction of the radar's wavelength.

The **Distributed Occluded Water Sensors using Electromagnetics in Reactive regime (DOWSER)** is a suborbital distributed polarimetric, MIMO (multi-input, multi-output) sounder concept. It uses quasi-static electromagnetic fields to advance detection and retrievals for deep subsurface groundwater where the high attenuation is prohibitive for remote sensing with traditional radar techniques. The distributed system improves the localization and detection of subsurface features.

Background

DEBRIS synthesizes antenna apertures that are physically large using synthetic aperture radar (SAR) techniques along-track and the distributed array beamforming creates the aperture in the across-track direction. By focusing the aperture in two-dimensions, we suppress the unwanted surface's echoes from off-nadir angles, and detect echoes from the subsurface at nadir. The relative spacing between the elements determines the shape of the synthesized antenna's sidelobes. The maximum extent of the array determines the horizontal resolution of the footprint. The number of elements impacts the aperture gain, and ultimately the sensitivity of the radar.

DOWSER provides enhanced suborbital resolution of deep subsurface targets, and 3D tomographic capability for high-attenuation environments with a coherent, distributed multi-sensor architecture. The current state-of-the-art relies on a single transmitter and receiver, which are moved (either together or separately) to spatially sample the environment. DOWSER introduces polarization and multiple receivers to improve both the measurement's spatial resolution and its accuracy.

Significance of Results/Benefits to NASA/JPL

Several science and application disciplines can benefit from the enhanced capabilities DEBRIS and DOWSER bring to subsurface remote observations. These include investigations in glaciers and ice sheets, desert aquifers, soil moisture, permafrost, and magmatic systems. Ice-sheet evolution, an area of research among the most consequential to sea level rise, requires observing dynamic changes where ice sounding is challenging because of steep topography (clutter) or the presence of melt water in or on the ice (high attenuation). DEBRIS significantly reduces surface clutter via a large antenna aperture to detect features in these challenging areas. DOWSER applies magneto- and electro-quasistatic techniques using low frequencies (typically <100's kHz) where the wavelength is greater than the investigation range. DOWSER uses tomographic techniques to image subsurface structures in high attenuation environments where radar cannot detect.

Approach and Results

Formation flying is critical to DEBRIS' performance. Its elements are allowed to maintain a relatively loose control (a fraction of their separation) but require accurate position knowledge for coherent operation (sub-wavelength). Passively safe orbital configurations were evaluated: a helical free-flying array, a linear array, and a tethered array aligned along nadir (Fig 1A). The helix formation provides separation in the cross-track direction throughout the orbit and demonstrates long-term system stability (Fig. 1C). A nadir-aligned formation of interconnected spacecraft can be constructed with a mechanical tether (a low mass cable) which is stable due to the gravity-gradient (Fig. 1E).

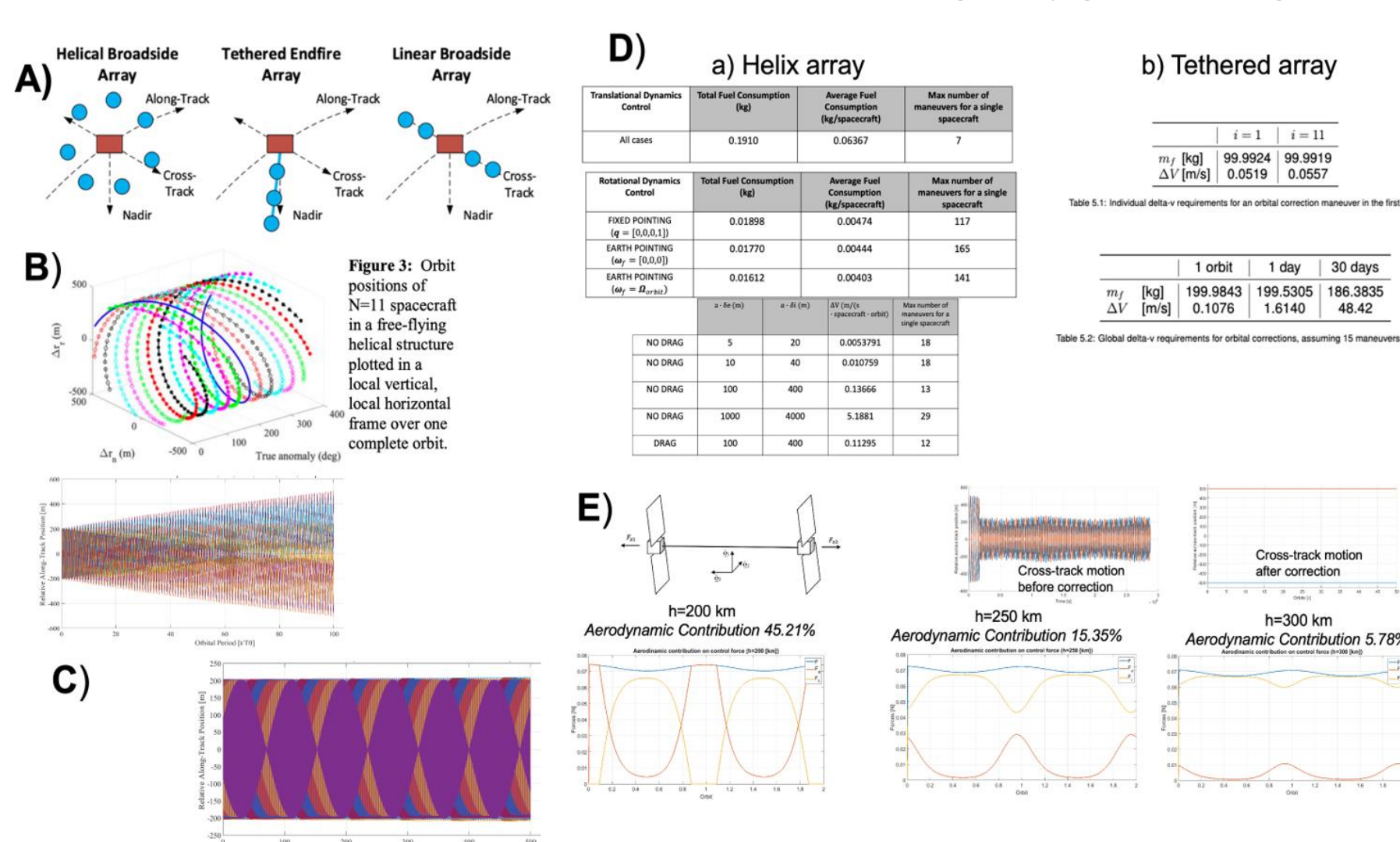


Figure 1: (a) Example of passively-safe orbital configurations considered for DEBRIS. (b) The relative positions of the array elements in a helix configuration with ten spacecraft orbiting in LEO. The formation requires periodic corrective maneuvers for position maintenance and collision avoidance. (c) Studies of long-term orbit stability were conducted. (d) Results of the orbit simulations, quantified in terms of fuel mass and delta V expended to maintain relative positions. (e) A novel configuration of aerodynamic surfaces was evaluated to use the atmosphere in LEO as a method stabilize a tethered cross-track geometry.

To implement the elements of the distributed radar array, deployable, dual-polarized, wide-band dipole antennas centered at 45 MHz are needed. We designed and fabricated such an antenna that is constructed from elliptical, stainless steel rings with a cover of gold-plated Kapton (Fig. 2). The antenna can be folded and stowed in a flat configuration (Fig. 2c) about one-third of its longest dimension and are deployed like a car sun-shade or a photography reflector. The response of the RF matching circuit was measured and agreed with the simulation model. The antenna range measurements demonstrated a return loss better than -10 dB over a band of more than 40 MHz at both polarizations with a center frequency of 70 MHz. While the matching network was improperly tuned for this test, the simulations and measurements agree. Simulation can be used to predict a retuned network and antenna's performance with high confidence.

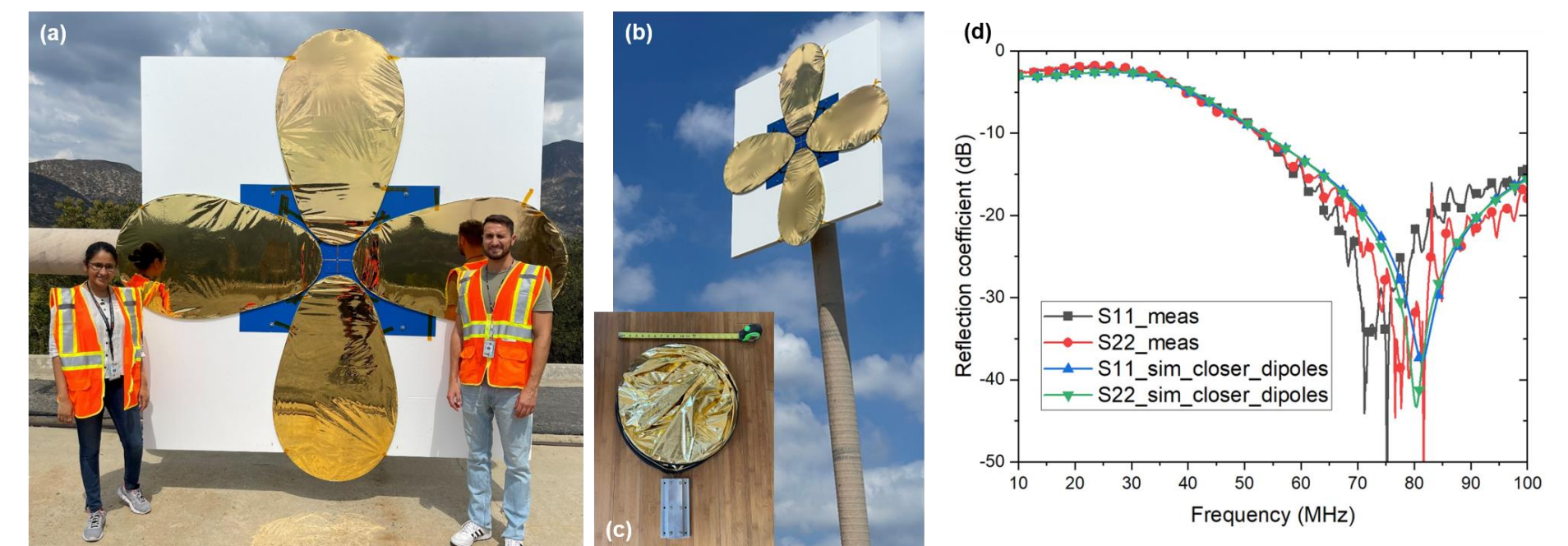


Figure 2: (a) A prototype dual-polarized VHF antenna mounted for testing at the JPL outdoor antenna range. The gold-plated Kapton antenna elements were mounted on a 8'x8'x3" layer of white EPS foam that is sandwiched between two blue G10 panels for mechanical support. (b) The VHF antenna raised above ground for testing. (c) Illustrative model of how the VHF antenna is folded and stowed. (d) The measured and simulated return loss of the antenna with matching network for both polarizations show good agreement. (Note the center frequency shift is due to an error in the tuned impedance.)

A detailed method of moments electromagnetic simulation of the DEBRIS spacecraft was developed in order to evaluate RF scattering and mutual coupling effects (Fig. 3a). Simulations show that spacecraft scattering can produce antenna pattern ripples that vary with array configuration and polarization. For a 400m diameter helix mutual coupling between antennas is typically less than -40dB. The ionosphere can also reduce performance through attenuation and phase scintillation at VHF, with simulations of attenuation suggesting an upper bound is approximately 1 dB (Fig. 3b).

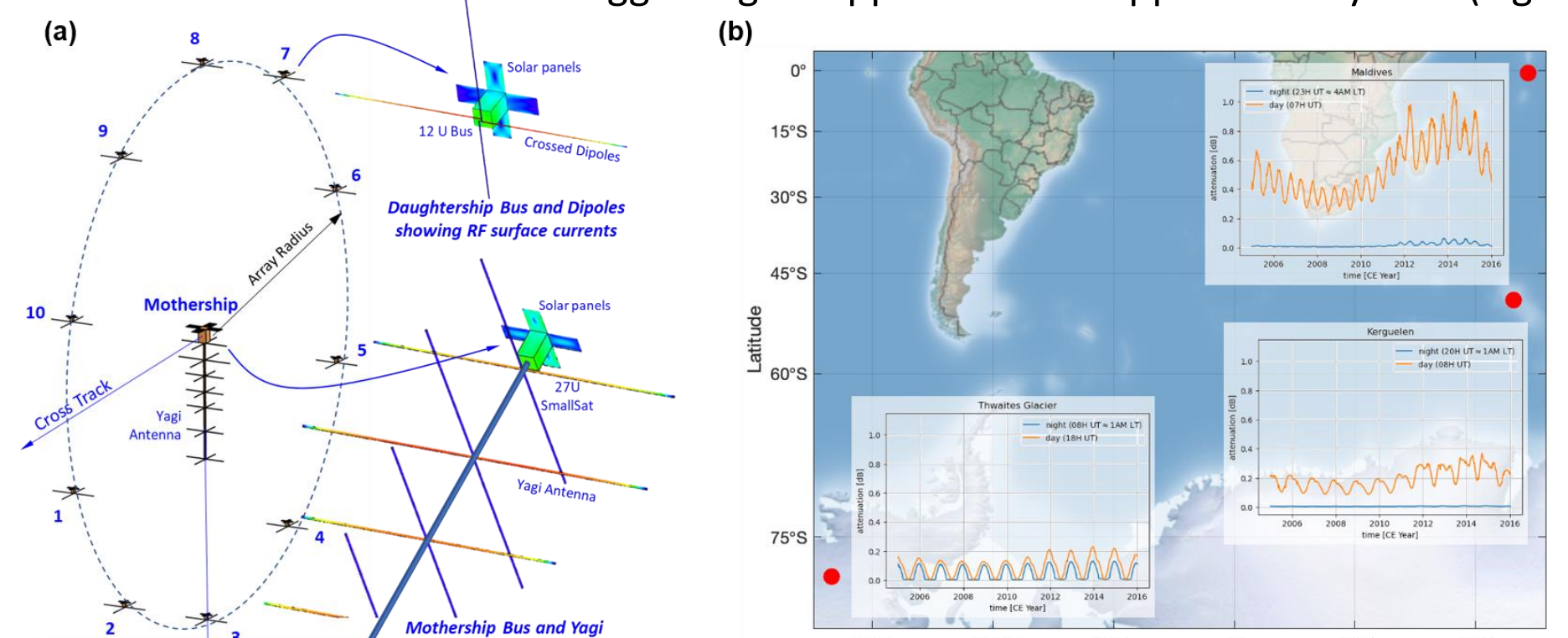


Figure 3: (a) Method of Moments model of a nominal DEBRIS spacecraft configuration used to evaluate array RF scattering and mutual coupling effects. Illustration shows a 27U Mothership with 12dB gain Yagi (transmitter), and ten 12U Daughterships with crossed dipoles (receive array). A circular ring array was used for simplicity, but the model can handle any orbital spacecraft configuration. Enlarged images of the Mothership and Daughterships show details of the spacecraft models and induced RF surface currents. (b) Estimates of two-way attenuation in the ionosphere for a 45 MHz sounding radar. Up to 1 dB of loss to be allocated for ionosphere attenuation.

The relative position, timing and frequency estimates can be met using GPS. The radiometric accuracy of the array elements and polarimetric alignment are also important to sidelobe suppression during array synthesis. The 2D patterns (Fig. 4b) are distilled into gain curves to compare arrays configuration in Fig. 4c. Array sidelobe errors are shown in Fig. 4d for one case using effective timing errors.

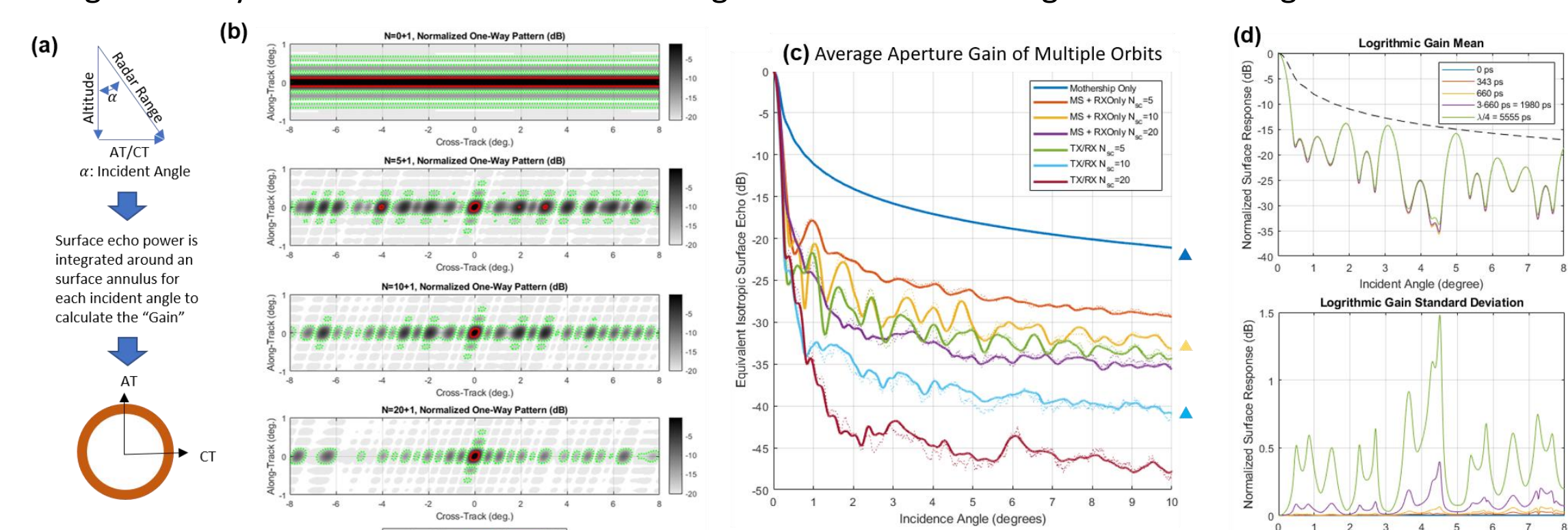


Figure 4: The array's configuration evolves through the orbit resulting in different sampling of the aperture. The effective antenna pattern varies as a result. (a) The 2D pattern is reduced to a gain curve by integrating iso-ranges and converting to angles. (b) Example 2D antenna patterns after pattern synthesis. (c) Illustrates the relative, mean clutter response for: single spacecraft, RX-only arrays and full TX/RX arrays. Compared to the single SAR spacecraft: ~10 dB improvement in SCR for 10 S/C RX-only array plus Mothership, and ~20 dB improvement in SCR for 10 S/C full-TX/RX array. CT diameter starting at 800 m and evolving to 1300 m over approximately 7 days. (d) Illustrates the mean and standard deviation of array uncertainty, in the form of equivalent timing error, for a ten-Daughtership receive-only array plus RX/TX Mothership for one configuration. The dashed black line is the equivalent single spacecraft SAR gain.

The DOWSER team has developed a prototype system based on the findings from simulation and bench measurements to detect conductive bodies ~100 m below the surface (Fig. 5). This prototype system has been verified in a lab environment with validation of functionality of both the transmitting and receiving subsystems and are ready for field testing.

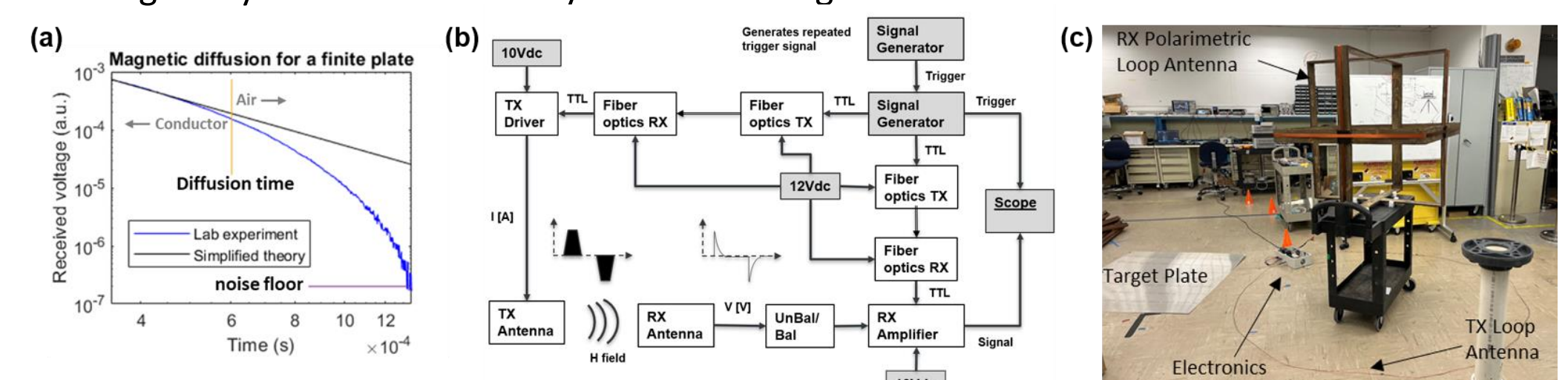


Figure 5: (a) Comparison of theoretical and lab test results for a plate target to verify the system concept. (b) Schematic block diagram of the DOWSER system. (c) Image of the DOWSER prototype system in the lab with a target plate for testing.

Publications

- [A] Mazouz, R., Quadrelli, M., Beauchamp, R., "Dynamics and Optimal Control for Free-Flight and Tethered Arrays in Low Earth Orbit", IEEE Aerospace Conference, 2021.
 [B] Haynes, M., Beauchamp R., Khazendar, A., Mazouz, R., Quadrelli, M., Focardi, P., Hodges, R., Bertiger, W., Bienert, N., "DEBRIS: Distributed Element Beamformer Radar for Ice and Subsurface Sounding," IEEE IGARSS 2021.
 [C] Apa, R., Quadrelli, B.M., Beauchamp, R., "Dynamics and Control of Helical Arrays in Low Earth Orbit", IEEE Aerospace Conference, 2022.
 [D] Pastori, M., Braghin, F., Quadrelli, B.M., Beauchamp, R., "Modeling, Dynamics, and Control of Variable Topology Tethered Space System", IEEE Aerospace Conference, 2022.
 [E] Mazouz, R., Mao, P., Quadrelli, B.M. Beauchamp, R., "Dynamics and Control of Precise Pointing and Collision Avoidance of an Array of Distributed Spacecraft", 11th International Workshop on Satellite Constellations & Formation Flying, 2022.
 [F] Apa, R., Mao, P., Quadrelli, B. M., Beauchamp, R., "Effective Sensitivity Analyses of Radar Systems in Formation Flying using Differential Algebra", 11th International Workshop on Satellite Constellations & Formation Flying, 2022.
 [G] Focardi, P., Beauchamp, R. M., Horst, S. J., Lavalle, M., Nunes, D. C., Shenoy, T.: "Wide-band Planar Dipole Antennas for Earth and Planetary Applications", WAMS 2022.
 [H] Bienert, N., Haynes, M., Schroeder, D., Beauchamp, R.: "SFMW Orthogonal Wave Beamforming Concept for Distributed Orbital Sounding", IEEE IGARSS 2022.

National Aeronautics and Space Administration
 Jet Propulsion Laboratory
 California Institute of Technology
 Pasadena, California
www.nasa.gov

PI Email: robert.m.beauchamp@jpl.nasa.gov
 Clearance Number: CL#22-5465
 Poster Number: RPC-092
 Copyright 2022. All rights reserved.